Colloid & Polymer Science Colloid Polym Sci 272:619–632 (1994)

Leading Contribution

A model for cation adsorption to clays and membranes

S. Nir[1]), G. Rytwo[1]), U. Yermiyahu[1]), and L. Margulies[1])

The Seagram Center for Soil and Water Sciences, Faculty of Agriculture, The Hebrew University of Jerusalem, Rehovot, Israel

Abstract: A cation adsorption model is presented and its recent applications are discussed. The model combines electrostatic equations with specific binding, and considers neutral and positively charged complexes between the negative surface sites and organic cations in a closed system. Extensions in the model account for dye aggregation in solution, and for the formation of solution complexes of inorganic cations, such as $[M^{++}Cl^{-}]^{+}$. The amounts of $45Ca^{2+}$ adsorbed to vesicles extracted from the plasma membranes of melon root cells could be adequately simulated and predicted. The binding coefficients determined for Ca^{2+}, Na^{+}, and Mg^{2+} are in the range of values previously deduced for binding to phospholipid vesicles. However, a large fraction of the bound Ca^{2+} is due to non-phospholipid components. Model calculations were applied to the test of hypotheses on the effect of salt stress on the growth of roots. The adsorption of monovalent organic cations to montmorillonite is characterized by binding coefficients that are at least six orders of magnitude larger than those of Na^{+}, Mg^{2+}, Ca^{2+}, and Cd^{2+}, or those of $CdCl^{+}$ or $CaCl^{+}$. Monovalent organic cations were found to adsorb 140–200% of the cation exchange capacity of the clay and to cause charge reversal. Deductions from adsorption results of acriflavin are consistent with those drawn from the application of other experimental methods. Preliminary results on the adsorption of divalent organic cations are presented. Agro-environmental applications of organo-clays are discussed.

Key words: Cation adsorption – Ca^{2+} binding to membranes – organic cation adsorption – cation complexation and adsorption

Introduction

This article presents a model for cation adsorption [1–4] whose recent applications have included Ca^{2+} adsorption to bile salt micelles [5], reexamination of the adsorption of Ca^{2+} and Mg^{2+} to montmorillonite [G. Rytwo, A. Banin and S. Nir, unpublished], Ca^{2+} adsorption to vesicles extracted from plasma membranes of root cells [6], and adsorption of monovalent organic cations to montmorillonite [4]. We also present here a few results on the adsorption of a divalent organic cation to montmorillonite when added alone, or in competition with a monovalent organic cation. Each of these applications necessitated a particular development in the equations of the model, or in the computational procedure, which will be described here.

Three main elements characterize the adsorption model [1, 2]: i) Specific binding; the total amount of cations adsorbed is assumed to consist of a) cations tightly bound to the surface and b) cations residing in the double-layer region; ii) The electrostatic Gouy–Chapman equations are solved for a solid-liquid system containing several cations of various valencies interacting with particles whose surfaces are charged and partially neutralized by cation binding; and iii) The concentration of surface sites is explicitly taken into account since it affects the concentration of non-adsorbed cations remaining in solution. The concentration of free cations in solution may be

reduced by several orders of magnitude as a result of cation adsorption to the particles.

Measurements of adsorbed amounts of cations involve the application of several experimental procedures, such as the measurement of radioisotopes and atomic absorption of adsorbed cations or cations remaining in solution [3–10], ICPES (inductively coupled plasma emission spectroscopy [11]), nuclear magnetic resonance [12–14], electrokinetic measurements [15–16], and surface potential measurements [17]. All these methods yielded mutually consistent results. Furthermore, the information deduced from adsorption studies can be used in interpretations of results of infrared absorption [4, 18], linear dichroism [4], UV and visible spectra [4], and x-ray scattering [4, 19]. As will be demonstrated, model calculations can play a crucial role in providing estimates of adsorbed amounts of cations, and surface charge densities and potentials for situations where experimental determinations are impossible. We will demonstrate the usefulness of model calculations in tests of hypotheses on biological systems and in ecological applications, such as formulations of pesticides [20].

Experimental

Materials

The clay mineral used was Wyoming Na-montmorillonite SWy-1 obtained from the Source Clays Repository of The Clay Minerals Society. The CEC of this clay was reported to be 0.764 mmol g^{-1} [25], and its specific surface area (SSA) as 756 $m^2 g^{-1}$ [26]. Paraquat (PQ) was obtained from Sigma (Sigma Chemical Co., St. Louis, Missouri USA). Acriflavin (AF) was obtained from Fluka Chemica (Fluka Chemie AG, Buchs, Switzerland). Both materials were received as chloride salts, and were used without further treatment or purification.

Adsorption isotherms

To measure adsorption isotherms of PQ, aliquots of an aqueous 0.5×10^{-2} M solution of dye were added dropwise under continuous stirring to 20 mL of a 0.5% w/w clay mineral suspension in 100 mL polyethylene bottles. The final volume was brought up to 60 mL. The bottles were sealed and kept at 25 ± 1 °C under continuous agitation. The adsorption of PQ was found to be almost unaffected in the range of pH between 4.5–8.5 [27]. The pH measured was between 6.92 and 7.45 for all samples during the adsorption process. After various times of incubation 10 mL of suspension were taken from each bottle and filtered through S&S FP030/2 disposable filters (Schleicher & Schuell, Dassel, FRG), with 0.45 μm pore diameter cellulose acetate membranes.

The concentration of the dye in the filtrates was determined by measuring the adsorption at 258 nm (PQ, $\varepsilon = 20500\ M^{-1} cm^{-1}$) using a HP 8452A diode array UV-Vis spectrophotometer (Hewlett–Packard Company, Scientific Instruments Division, 1601 California Avenue, Palo Alto, California, USA). The limit of detection for the dye (as defined to yield an optical density of 0.01) was 4.9×10^{-7} M. Experiments were carried out in triplicate.

Competitive adsorption

Aqueous 1×10^{-2} M solutions of PQ and AF were prepared. Equal volumes of pairs of dyes (PQ and AF) were mixed so that the aqueous solutions contained 1×10^{-2} N of each dye, e.g., 1×10^{-2} M of AF and 0.5×10^{-2} M of PQ. Aliquots of these solutions were added to the silicate suspension as described above. Separation and spectroscopic measurements were made after 1, 6, and 12 days.

Measurements were performed as above. The concentration of AF in the filtrates was determined by measuring the absorption at 450 nm ($\varepsilon = 37200\ M^{-1} cm^{-1}$). The spectra were decomposed mathematically into those of the individual components, which allowed to determine the concentration of each dye. The correlation found with the spectrum of each dye alone was higher than 0.99, indicating that there was no chemical interaction between the two dyes in the solution that might affect their spectra.

Linear Dichroism Infrared (LDIR) spectra

Aliquots of an aqueous 1×10^{-2} M dye solution were added dropwise under continuous stirring to 5 mL of a 0.5% suspension of SWy-1

montmorillonite in 20-mL bottles. The amount of dye varied from 0 to 1.2 mmole dye g^{-1} clay. The final volume was brought to 15 mL with distilled water. The bottles were shaken for 24 h at 25 ± 1 °C. One mL of each suspension was diluted with 10 mL of distilled water in glass test tubes. The tubes were sonicated for 5 min in an ultrasonic bath. From the tubes containing 0, 0.2, 0.6, and 1.2 mmole dye g^{-1} clay, 2 mL were sampled and dropped gently on ZnS (Irtran-2) plates. The dye-silicate complex was allowed to sediment for 3 days in closed petri dishes. Then, the cover was partially opened, allowing the water to evaporate for 4 more days. Another 2 mL of the respective suspension were dropped on the plate, and the process was repeated once again, to create a layer of approximately 12 μm. From each sample, three FTIR spectra were measured as described in [28]: one using unpolarized light at normal incidence; and two polarized light spectra (LD 0 ° and LD 90 °). The latter two spectra were used to analyze clay orientation and dye orientation over the clay plates [28–30]. Spectra were measured with a Nicolet MX-S spectrophotometer, (Nicolet Analytical Instruments, 5225–1 Verona Road, P.O. Box 4508, Madison, Wisconsin, USA). Spectra of the dyes ("free" dyes) were measured using a KBr pellet containing 1% dye.

Theoretical

Adsorption model

Notations: X_i^+ denotes a monovalent cation that binds to singly charged negative sites, P^-, on the surface of the silicate, or membrane:

$$P^- + X_i^+ = PX_i\,. \tag{1}$$

The binding coefficient for such reaction, K_i, is,

$$K_i = [PX_i]/([P^-][X_i(0)^+])\,, \tag{2}$$

in which $[X_i(0)^+]$ is the concentration of the cation at the surface. Divalent cations can form a 1–1 charged complex with a binding coefficient K_{j1} and a 2–1 neutral complex with a binding coefficient K_{j2}.

The 1–1 complexation is described by:

$$P^- + X_i^{++} = PX_i^+ \tag{3}$$

$$K_{j1} = [PX_i^+]/([P^-][X_i(0)^{++}])\,. \tag{4}$$

For the 2–1 complexation, we formally define a divalent site, P^{--}. The concentration of such sites is $P^-/2$.

$$P^{--} + X_i^{++} = PX_i \tag{5}$$

$$K_{j2} = [PX_i]/([P^{--}][X_i(0)^{++}]) = [PX_i]/(([P^-]/2)[X_i(0)^{++}])\,. \tag{6}$$

Organic monovalent cations can form charged complexes with the clay:

$$PX_i + X_i^+ = P(X_i)_2^+\,, \tag{7}$$

with a binding coefficient $\bar{K}_i$:

$$\bar{K}_i = [P(X_i)_2^+]/([PX_i][X_i(0)])\,. \tag{8}$$

In Eqs. (2), (4), (6) and (8) the concentration of the cation close to the silicate layer is needed. We employ the relation:

$$Xi(0) = XiY(0)^{z(i)}\,, \tag{9}$$

where $Y(0) = \exp(-e\phi(0)/kT)$, e is the absolute magnitude of an electronic charge, Z_i is the valence of the given ion, $\phi(0)$ is the surface potential, k is Boltzmann's factor, T is the absolute temperature, and Xi is the molar concentration of cation i in its monomeric form in the equilibrium solution, far away from the surface.

For a negatively charged surface $Y(0) > 1$, and the concentration of the cation at the surface, $X_i(0)$, may be significantly larger than Xi. If charge reversal occurs, however, $\phi(0)$ is positive and $Y(0) < 1$. Here, the concentration of non-adsorbed cations in the double layer region may be significantly smaller than their solution concentration.

If we ignore the formation of mixed complexes, the total concentration of the monovalent cation i, $C_{tot}(i)$, is given by:

$$C_{tot}(i) + Xi + PX_i + P(X_i)_2^+ + D_{lp}(i)\,. \tag{10}$$

$D_{lp}(i)$ represents the excess concentration of cation i in the double layer region above the bulk concentration, Xi. A simplifying assumption is that all cations of the same valency behave similarly in the double layer region. Thus, a proportion factor Q_J can be defined for each valency J,

and $D_{lp}(i)$ is proportional to the ratio between the concentration of cation i and the sum of all concentrations of J-valency cations:

$$D_{lp}(i) = Q_J \cdot \frac{Xi}{\sum Xi(J)} . \quad (11)$$

The quantities Q_J can be obtained analytically, when the system includes only mono and divalent cations, and one type of anions [8]. A numerical integration provides Q_J in the general case [4].

The intrinsic surface charge density, σ_{in}, is given by the charge of all surface sites, i.e., by the ratio of the cation exchange capacity (CEC) to the specific surface area of the clay mineral (SSA). For instance, the area per surface site of the clay employed by us [4] is 1.55 nm^2. The total site concentration, PT, equals the sum of concentrations of all sites, free and complexed. The actual surface charge density, σ, depends on the amount of free sites on the clay mineral. In the absence of charged complexes, the following ratios hold:

$$\frac{\sigma}{\sigma_{ini}} = \frac{P^-}{PT} = \frac{P^-}{P^- + \sum PX^0} , \quad (12)$$

where $\sum PX^0$ is the sum of all neutral complexes, i.e.,

$$\sum PX^0 = \sum PX(i^+) + 2 \cdot \sum PX(i^{2+}) + 3 \cdot \sum PX(i^{3+}) + 4 \cdot \sum PX(i^{4+}) . \quad (13)$$

In cases where charged complexes may exist, positively charged complexes decrease the negative value of σ. If $\sum PX^+$ is the sum of all positively charged complexes, then Eq. (12) becomes:

$$\frac{\sigma}{\sigma_{in}} = \frac{P^- - \sum PX^+}{P^- + \sum PX^0 + \sum PX^+} . \quad (14)$$

In Eq. (14) the possibility of charge reversal arises when $P^- < \sum PX^+$.

The continuity relation between the electrostatic surface potential and the surface charge density is:

$$\frac{d\phi}{dx} = \frac{4\pi\sigma}{\varepsilon} . \quad (15)$$

The Gouy–Chapman equation yields for σ:

$$\sigma^2 = \frac{\varepsilon kT}{2\pi} \sum n_i(\infty)(Y(0)^{z(i)} - 1) = \frac{1}{G^2} \sum X_i (Y(0)^{z(i)} - 1) , \quad (16)$$

where ε is the dielectric coefficient of the medium, and G depends on T, ε, and the system of units (see [1, 21]).

For the case of 1, 2, 3, and 4 valent cations, and mono and divalent anions, the combination of Eqs. (14) and (16) gives a polynomial equation for $Y(0)$. The solution has been obtained by numerical procedures. In certain limiting cases of no binding, where all ions have the same valency, analytical solutions are also available.

These equations form a closed set. Thus, Eq. (10) may yield the values Xi, if $Y(0)$ and P^- are known. Equation (12) may yield a solution for P^-, if the different Xi and $Y(0)$ are known. The combination of Eqs. (14) and (16) may give a value for $Y(0)$, if Xi and P^- are known. The equations can be solved iteratively by the following procedure:

1) An initial value for $Y(0)$ and P^- is assumed.
2) The values of Xi are calculated by using Eqs. (10) and (11).
3) A new value of $Y(0)$ is obtained by using Eqs. (14) and (16)
4) A new value is obtained for P^- using Eq. (12).
5) Another iteration starts from stage 2.

The iteration steps may be continued until the desired degree of convergence is reached.

The model presented is amenable for extensions. For example, certain organic cations can form aggregates in solution [22, 23]. Expressions for the general distribution of aggregates [24] yield that the total concentration of primary dye molecules in solution, Xi_t, is given by:

$$[Xi_t] = [Xi]/(1 - K_{ag} \cdot [Xi])^2 , \quad (17)$$

in which K_{ag} is the corresponding binding coefficient for aggregation in solution. In our treatment [4], K_{ag} was determined from the absorption spectrum of the dyes alone in solution.

Aggregation of dye molecules reduces the concentration, Xi, of dye monomers. For the specific case of methylene blue, we ignored the adsorption of dye dimers or higher order aggregates. Accounting for the binding of dye aggregates amounts to the addition of more adjustable parameters, which were not needed for the simulation of the adsorption results [4]. It may be noted that the influence of dye aggregation in solution can only occur when its total added amounts are

above the CEC of the clay, since below the CEC essentially all the dye adsorbed [11].

In the general case, when more than a single organic monovalent cation interacts with the clay, mixed complexes involving one clay binding site, one molecule of cation i and a molecule of cation j can exist. Such charged mixed complexes would be described by the reactions:

$$PX_i + X_j^+ = PX_iX_j^+$$
$$PX_j + X_i^+ = PX_jX_i^+ , \quad (18)$$

and

$$K_{ij} = [PX_{ij}^+]/([PX_i][X_j(0)])$$
$$K_{ji} = [PX_{ji}^+]/([PX_j][X_i(0)]) . \quad (19)$$

The additional binding coefficients are not symmetrical, i.e., $K_{ij} \neq K_{ji}$.

In all equations the concentrations are given in units of mole L^{-1}, or M; and the unit of K_i or $\bar{K}_i$ is M^{-1}.

Another extension of the model enables to account for formation of solution complexes of the type $[M^{++}A^-]^+$, where A^- designates an anion. In the case of Cd^{2+} it was also needed to consider neutral complexes in solution, such as $CdCl_2$. The charged complexes were considered in the equations as cations of the respective valency, whereas the neutral complexes were assumed not to adsorb. A detailed description of this extension is given in [3].

Results and discussion

Adsorption of Ca^{2+} to biological membranes

Adsorption or binding of Ca^{2+}, Mg^{2+} and Na^+ to model membranes consisting of phospholipids has been widely studied [1, 7, 9, 12, 14, 16–19, 24, 31–36]. We have recently studied the sorption of $^{45}Ca^{2+}$ to plasma membrane (PM) vesicles of melon roots in the presence of a wide range of concentrations of Ca^{2+}, Na^+ and Mg^{2+} [6]. The ultimate goal of this study is to test hypotheses about salinity stress and characterization of salt resistant cultivars.

Calcium plays a structural role in cell membranes by preventing damage and leakage [37]. Leakage of K^+ from cells in high-salt solutions is a well-established phenomenon [38–40]. The presence of Ca^{2+} has been shown to prevent K^+ leakage from cultured citrus cells under saline conditions [40]. In that study, the initial change in membrane permeability was attributed to displacement of membrane-associated Ca^{2+} by Na^+.

The effect of competition between Ca^{2+} and Na^+ and Ca^{2+} and Mg^{2+} on Ca^{2+} adsorption to PM vesicles is illustrated in Tables 1 and 2, respectively. In the following, we explain the steps involved in the application of the model to biological membranes.

The program [1] calculates the solution and sorbed concentrations of each cation, in this case Na^+, Ca^{2+}, and Mg^{2+}. The sorbed concentration consists of cations tightly bound to the surface sites and cations residing in the double-layer region close to the negatively charged surfaces. The input consists of i) the total concentration of each cation, ii) the concentration of surface sites, and iii) the area per non-neutralized charged site. In our case, the binding coefficients (K_{Na}, K_{Ca}, and K_{Mg}) were considered constant parameters whose magnitudes were determined from the best agreement between the experimental and calculated values of the amount of Ca^{2+} sorbed for various total concentrations of Na^+, Ca^{2+}, and Mg^{2+}.

Table 1. Number of sorbed Ca^{2+} ions per charged site (Ca/e) on PM vesicles of melon roots as a function of total concentrations of Ca^{2+} and Na^+ added

Treatment Ca^{2+} (mM)	Treatment Na^+ (mM)	Experimental sorbed [1] (ion/charge)	Calculated sorbed [1] (ion/charge)	Calculated bound [2] (ion/charge)	$-\phi(0)$ (mV)
0.05	1	0.107 ± 0.007	0.137	0.129	142.0
0.05	20	0.057 ± 0.007	0.081	0.076	67.7
0.05	40	0.035 ± 0.005	0.047	0.045	54.6
0.05	100	0.009 ± 0.003	0.017	0.016	38.0
0.5	1	0.388 ± 0.014	0.454	0.343	61.6
0.5	20	0.235 ± 0.012	0.264	0.236	49.2
0.5	40	0.181 ± 0.011	0.195	0.180	43.2
0.5	100	0.111 ± 0.011	0.105	0.100	33.2
1.0	1	0.500 ± 0.022	0.470	0.350	50.6
1.0	20	0.350 ± 0.017	0.312	0.272	42.6
1.0	40	0.261 ± 0.008	0.247	0.224	38.0
1.0	100	0.202 ± 0.011	0.155	0.146	30.2

[1]) Sorbed Ca^{2+} includes the cations bound at the surface plus the amount of the cations in the diffuse double-layer region

[2]) Bound represents only cations chemically bound to the surface

Table 2. Number of sorbed Ca^{2+} ions per charged site (Ca/e) on PM vesicles of melon roots as a function of total added concentrations of Ca^{2+} and Mg^{2+}

Treatment Ca^{2+} (mM)	Treatment Mg^{2+} (mM)	Experimental sorbed [1] (ion/charge)	Calculated sorbed [1] (ion/charge)	Calculated bound [2] (ion/charge)	$-\phi(0)$ (mV)
0.01	2.0	0.004 ± 0.001	0.007	0.006	52.7
0.1	0	0.209 ± 0.031	0.268	0.242	121.8
0.1	0.1	0.165 ± 0.017	0.231	0.197	89.9
0.1	0.5	0.101 ± 0.010	0.137	0.117	67.6
0.1	1.0	0.075 ± 0.006	0.094	0.081	59.3
1.0	0	0.500 ± 0.052	0.470	0.350	50.6
1.0	0.5	0.440 ± 0.042	0.390	0.300	47.5
1.0	1.0	0.393 ± 0.036	0.340	0.270	45.1
1.0	5.0	0.199 ± 0.019	0.180	0.155	35.5

[1]) Sorbed Ca^{2+} includes the cation bound at the surface plus the amount of the cations in the diffuse double-layer region
[2]) Bound represents only cations chemically bound to the surface

This procedure of determination of binding coefficients has been applied to model systems [1, 8, 9, 12, 17]. In those cases, the concentrations of cations in solution were experimentally known. Applications to closed systems, where the concentrations of cations in solutions are not known *a priori*, are given in [1, 5, 10, 29]. The situation existing in sorption studies on biological membranes in more complex.

Unlike studies on model membranes or clays, the concentration of surface sites and the area per charged site are currently unknown for biological membranes. We approximated the surface charge by using an effective concentration of charged sites and an effective area per site. The effective concentration of charged sites was found from the case in which no Na^+ had been added and Ca^{2+} concentration was 1 mM. In this case, irrespective of the parameter values, the surface is assumed to be saturated and neutralized by Ca^{2+}. Experiments [41] ruled out charge reversal under these conditions. This means that the experimental ratio of Ca^{2+} (sorbed) per site should be equal 1/2. Our measurements gave the amount or concentration of Ca^{2+} sorbed; thus the concentration of charges sites was fixed. We considered 2–1 binding modes of Ca^{2+} and Mg^{2+} (Eqs. (5) and (6)).

In estimating the surface area per site, we considered a range of values from 0.50 nm^2 to 6 nm^2. For each chosen value of the surface area, we determined the parameters K_{Ca} and K_{Na} that gave the best agreement between the calculated and experimental values of sorbed Ca^{2+}. We then chose the value of surface area per site that gave the best agreement between the experimental and calculated values of the amounts of Ca^{2+} sorbed. The value of the effective surface area per site was found to be 3.7 nm^2 ($\pm$ 0.3 nm^2). The binding coefficients used for K_{Ca}, K_{Na}, and K_{Mg} were 50, 0.8, and 9 M^{-1}.

Tables 1 and 2 illustrate that experimentally determined amounts of Ca^{2+} sorbed to the PM vesicles agreed fairly well with those calculated with the sorption model which took into account specific binding to surface sites and the amount of cations in the electrical double layer. The model also calculated the effect of surface site concentration on the degree of sorption and took into account the depletion of cations from the solution as a result of sorption.

A salt resistant cultivar yielded a larger amount of Ca^{2+} sorbed per given amount of protein. However, the area per charge and binding coefficients turned out to be the same for both cultivars. The electrophoretic mobility of PM vesicles measured by free-flow electrophoresis was the same for the two cultivars (U. Yermiyahu, S. Nir, G. Ben-Hayyim, U. Kafkafi, and G.F.E. Scherer, unpublished). The electrophoretic mobilities yielded zeta potentials in accord with the predictions, namely, about 20 mV below the calculated absolute values of the surface potentials. The binding constants used in this study were in the range of previously reported values for phospholipid vesicles obtained by different methods [1, 8, 9, 12, 15–17, 21, 35], indicating that the behavior of biomembranes resembles that of phospholipid bilayers. However, our results indicated that non-phospholipid components in the PM contribute significantly to Ca^{2+} binding.

To gain a better understanding of the relations between root elongation and the amount of Ca^{2+} bound to the PM, melon plants were grown in an aerated solution which contained different concentrations of Ca^{2+} with various levels of Na^+, Mg^{2+}, or mannitol. With increasing external concentrations of NaCl, $MgCl_2$ or mannitol, the roots showed suppression of elongation. Addition of $CaCl_2$ to the external medium alleviated the inhibition of root elongation under high concentrations of Na^+, Mg^{2+}, but not mannitol. Root

elongation for 72 h under high levels of NaCl or $MgCl_2$ was correlated with the amount of Ca^{2+} bound to the PM. A model describing inhibition of root elongation was developed. This model took into account the effect of osmotic pressure in the growth solution (based on the mannitol experiments) and the effect of the amount of Ca^{2+} bound to the PM. The amount of Ca^{2+} bound to the PM was calculated by applying the sorption model using the same parameters deduced from PM vesicles.

It must be noted that a direct determination of the amount of Ca^{2+} adsorbed by the roots was impossible. Thus, model calculations were essential for correlating growth inhibition with adsorbed amounts of Ca^{2+}.

The model for inhibition of root elongation yielded a critical value of Ca^{2+} ions bound to the PM which is necessary for maximal root elongation. A decrease from this critical value gives a linear increase of the percent inhibition with a decrease in the amount of Ca^{2+} bound to the PM. In the case of the cultivar corresponding to Table 1 (in NaCl solution), it was established that as long as the fraction of Ca^{2+} bound per charge was 0.29 or more, root elongation was not inhibited (U. Yermiyahu, S. Nir, G. Ben-Hayyim, and U. Kafkafi, unpublished).

Adsorption of Cd^{2+}, Ca^{2+} *and* Mg^{2+} *to montmorillonite*

An implicit assumption in the model calculations [1, 2, 8, 16, 17, 21, 42] has been that only the valency of the anion in solution affects the amounts of cations adsorbed. This assumption is indeed valid when studying the adsorption of most monovalent cations. However, in the case of Cd^{2+}, which can form complexes in solution, such as $CdCl^+$ and $CdCl_2$, even at micromolar concentrations, the choice of a particular anion can modify the amount of cadmium adsorbed.

The perchlorate ion (ClO_4^-) is a weak ligand that does not form complexes with Cd or other metal ions, except in extremely concentrated perchloric acid. On the other hand, the association constants for the complexes $CdCl^+$ and $CdCl_2$ are $10^{1.98}$ M^{-1} and $10^{2.6}$ M^{-2}, respectively [43]. The adsorption of Cd to montmorillonite is significantly reduced if Cl^- replaces ClO_4^- in solution (see Table 3).

Table 3. Observed and calculated adsorption of Cd^{2+} to montmorillonite in solutions of $NaClO_4$ or NaCl at various ionic strengths

$NaClO_4$(M)	Cd_T(μM)	% Cd adsorbed	
		Observed	Calculated
0.01	0.27	97.3	98.1
	0.80	96.3	98.1
0.05	0.27	92.3	85.8
	0.80	87.8	85.8
NaCl(M)			
0.01	0.27	92.3	96.5
	0.80	94.3	96.5
0.05	0.27	48.3	43.5
	0.80	42.2	43.5

Experimental data are taken from [3]. See [3] for a more complete set of cases and details. The binding constants used are 1, 10, and 30 M^{-1} for Na^+, Cd^{2+} and $CdCl^+$. The area per site is 1.4 $(nm)^2$/charge and the adsorbing site concentration is 2.05 mM. Cd_T is the total concentration of cadmium ions in the system

In the calculations, we have employed $K_{Na} = 1\ M^{-1}$ [10], $K_{Cd} = 10\ M^{-1}$, and $K_{CdCl+} = 30\ M^{-1}$ [3].

In our study on the adsorption of Ca^{2+} and Mg^{2+} to montmorillonite (G. Rytwo, A. Banin, and S. Nir, unpublished), we have determined the amounts of adsorbed cations by a single incubation of the clay in a suspension containing a low concentration of an organic cation of large binding affinity, followed by analysis of the displaced cations by inductively coupled plasma emission spectrometry (ICPES) [11]. This procedure enabled to significantly increase the precision of adsorption measurements. The analysis of the results in the framework of the model is illustrated for the case of Mg^{2+} in Table 4. The calculations employed $K_{Na} = 1\ M^{-1}$ [10], and $K_{Mg} = 2M^{-1}$. It is evident that model calculations can simulate and quite well predict the amounts of Mg^{2+} and Na^+ adsorbed to montmorillonite, using constant binding coefficients for Na^+ and Mg^{2+}. This suggests that the binding affinity for Na^+ and Mg^{2+} is almost constant throughout the adsorption range studied here (0.0–0.9 of the exchange capacity).

A somewhat different behavior was observed for the Ca^{2+} adsorption isotherm in the Ca/Na system. At low concentrations of Ca^{2+}, a binding

Table 4. Adsorption of Mg^{2+} to montmorillonite

Total Na^+ concentration [M]	Total Mg^{2+} concentration [M]	Fraction of sites adsorbed by Na^+	Fraction of sites adsorbed by Mg^{2+} exp.	calc.
3.113E-02	1.094E-03	0.77	0.16	0.170
2.881E-02	5.034E-03	0.34	0.66	0.629
2.780E-02	7.549E-03	0.27	0.73	0.715
2.680E-02	1.007E-02	0.15	0.80	0.767
2.479E-02	1.513E-02	0.11	0.83	0.814
2.277E-02	2.011E-02	0.09	0.84	0.865
2.076E-02	2.518E-02	0.09	0.86	0.867
1.069E-02	5.034E-02	0.03	0.92	0.917

coefficient $K_{Ca} = 4\ M^{-1}$ could adequately simulate the experimental results. However, at higher Ca^{2+} concentrations, the calculated values of fractions of surface sites occupied by Ca^{2+} underestimated the experimental values. The simulation required the values of K_{Ca} to increase up to $30\ M^{-1}$ and above, as the total Ca^{2+} concentration increased.

Our proposal is that the enhanced binding affinity of Ca^{2+} to montmorillonite, which is observed for a larger fraction of surface occupation by Ca^{2+}, is largely due to the formation of a structure in which Ca^{2+} bridges two opposed surfaces. The chance for the formation of such structures increases as the fraction of the surface sites occupied by Ca^{2+} is increased.

The other possibility is that for closely apposed surfaces there is an increase in the magnitude of the surface potential, relative to the case of isolated surfaces, which in turn enhances the concentration of divalent cations relative to monovalent cations in the vicinity of the surfaces. In this context, it may be added that the hydration shells surrounding ions in solution are more tightly bound to Mg^{2+} (which has a smaller bare-ion crystallographic radius than Ca^{2+}) than they are to Ca^{2+}, in whose presence dehydration of closely opposed surfaces occurs. However, irrespective of the exact explanation for each system, the point is that the model described here has been shown in all cases to be applicable, whereas deviations in the direction of enhanced binding coefficients for certain divalent (or multivalent) cations can be anticipated for closely apposed surfaces.

In principle, it is hard to visualize that the macroscopic model of cation adsorption would hold for apposed surfaces at very small separations, e.g., of the order of atomic dimensions, although the formal extension of the electrostatic equations for interacting surfaces in a variety of geometries exists [44].

Experimental studies on phospholipid vesicles [45, 46] demonstrated that the affinity of binding of Ca^{2+} to PS increases dramatically in vesicles undergoing aggregation and fusion. Model calculations [1] showed the increase in the binding coefficient from 30 to $> 1000\ M^{-1}$ for such PS or PS/PE (1/1) vesicles of 50 nm radius. On the other hand, for similar PS/PC (1/1) vesicles that undergo aggregation but not fusion, a value of $K_{Ca} = 30\ M^{-1}$ could explain all the experimental results [1].

The calculations presented in Table 4 ignored the existence of a solution complex of the type $MgCl^+$ or $MgCl_2$. Similarly, we have performed calculations where such complexes were ignored for Ca^{2+}. For instance, the value listed in Lindsay [43] for the association constant of Ca^{2+} to $CaCl^+$ is $10^{-1}\ M^{-1}$, i.e., 1000–fold less than the corresponding association constant for Cd^{2+}. However, Sposito et al. [47] cite a larger value of the association constant, $10^{0.4}\ M^{-1}$, and advocated that in a chloride background of 50 mM, a great deal of the adsorption of Ca^{2+} and Mg^{2+} to montmorillonite arises from the adsorption of the monovalent cations $(M^{+}{}^{+}Cl^{-})^{+}$. These authors presented convincing evidence to support this proposal by showing that if such a possibility is ignored, then the apparent exchange capacity exceeds the CEC by up to 20 to 30% as the concentration of the divalent cation is increased at the expense of Na^+. Our calculations yield reasonably good predictions for the results of Sposito et al. [47] for the adsorption of Mg^{2+} and Ca^{2+} to montmorillonite in a perchlorate background of 50 mM by using the values of 1, 2 and $4\ M^{-1}$ for the binding coefficients of Na^+, Mg^{2+} and Ca^{2+}. We have also succeeded in fitting their adsorption data in a chloride background by employing a binding coefficient of $50\ M^{-1}$ for the adsorption of the monovalent complexes $MgCl^+$ and $CaCl^+$. Under these conditions, the calculated CEC for the chloride background was essentially independent of the concentrations of the divalent cations and its value was as in the perchlorate background. Nevertheless, the simulation of the data of Sposito et al. [47] on the

adsorption of Ca^{2+} also revealed that the calculated values underestimate the experimental amounts of Ca^{2+} adsorbed in the presence of larger Ca^{2+} concentrations (G. Rytwo, A. Banin, and S. Nir, unpublished). Hence, while the consideration of the monovalent complexes $(M^{++}Cl^{-})^{+}$ may be important, still the previously discussed phenomenon of an observed enhanced affinity of Ca^{2+} adsorption to PS vesicles also exists, though to a smaller degree, in Ca^{2+} adsorption to montmorillonite.

Adsorption of organic cations to montmorillonite

The nature of the various types of clay-organic interactions has been widely reviewed [48–53]. Several studies have reported on the adsorption of cationic organic dyes to negatively charged smectites [22, 27, 54–61].

We will first review results of studies with monovalent organic cations. Next, we will present a few of our recent adsorption results with a divalent organic cation, paraquat (PQ). The last subsection will describe the use of an organo-clay system in agro-environmental applications.

Monovalent organic cations

We have studied the adsorption of thioflavin T (TFT) [29], methylene blue (MB) [4, 29, 62], crystal violet (CV) [4, 62], and acriflavin (AF) on montmorillonite [4]. The binding coefficients, K_i, for the formation of neutral complexes with these cations [4, 29] are more than six orders of magnitude larger than those found for inorganic monovalent cations [3, 10].

Due to the strong binding affinity of monovalent organic cations to the clays, their addition in small concentrations resulted in an essentially complete displacement of inorganic cations such as Na^{+} or Ca^{2+} from the clay mineral. Model calculations indicating that three washes in 1 M solutions of ammonium acetate are less effective than a single application of a dilute concentration of CV were confirmed by analytical studies. Thus, the use of organic cations such as CV is suggested for the accurate determination of the CEC of clays, and the amounts of exchangeable inorganic cations [11].

Due to the formation of charged complexes via non-coulombic interactions between the organic ligands, the adsorption of all the above cations can exceed the CEC. The charge reversal predicted by the model beyond the CEC of the clay was confirmed by microelectrophoretic experiments. Particles loaded with amounts of organic cations below the CEC moved to the positive electrode, whereas a loading above the CEC resulted in a movement of the clay particles to the negative electrode [29].

The maximal amounts of CV, MB, AF, and TFT adsorbed are 200%, 150%, 175%, and $> 140\%$ of the CEC of the clay mineral, respectively. The model simulates the adsorbed amounts of the monovalent organic cations, and the competition between the cations for adsorption sites.

A survey of many studies on adsorption of inorganic cations to membranes [1, 8, 9, 35, 36] and clays [3, 10] shows that an increase in the ionic strength reduces adsorption of the cations studied, due to competition with the added cations, and due to a reduced magnitude of the (negative) surface potential (see also Tables 1 to 4). According to Eq. (19), the concentrations of cations near negatively charged surfaces are larger than their concentrations in bulk solution. In the case of adsorption of the monovalent organic cations MB and TFT to montmorillonite, their binding coefficients K_i are in the range of 10^8 to $10^9\ M^{-1}$, and $\bar{K}_i > 10^5\ M^{-1}$, in comparison with values such as $1–100\ M^{-1}$ for the inorganic cations. Thus, in the case of MB or TFT, an increase in the ionic strength to the 1 M range had practically no effect on their adsorption to montmorillonite below its CEC. However, Eq. (9) indicates reduced concentrations near the surface when adsorption occurs beyond the CEC, i.e., when $\phi(0) > 0$. The model thus predicted an enhanced adsorption of MB and TFT beyond the CEC with increased ionic strength, which causes a reduction in $\phi(0)$. Indeed, the saturation adsorption values of the dyes could be raised by 20–30% in media of ionic strengths approaching 1 M [29]. A similar effect of ionic strength was reported for the adsorption of AF [4].

In a recent study [4], we demonstrated that the adsorption model can play a central role in explaining results obtained with several experimental techniques, such as x-ray diffraction (XRD), UV and IR adsorption spectrocopies and IR linear dichroism (LDIR). Here, we discuss the case of AF.

Table 5 presents a few results of AF adsorption to montmorillonite. Model calculations yield reasonable simulations of the experimental results with the binding coefficients $K = 10^9\ M^{-1}$ and $\bar{K} = 6 \times 10^5\ M^{-1}$ (see Eq. (8)). It may be noted that up to the CEC all the dye added is adsorbed. Table 5 also shows the calculated fraction adsorbed as a charged complex.

Figure 1 shows the LDIR spectra of the clay-AF complexes. The difference between the different adsorption polarizations is 15–25% for a clay with 0.2 mmole AF/g and a clay with 1.2 mmole AF/g, and 10–15% for a clay with 0.6 mmole AF/g. From these results, we conclude that AF molecules lie parallel or almost parallel to the clay mineral plates [28, 30].

Table 5. Calculations of the fractions of dye molecules in the different species

Dye	Amount added [mmole g^{-1}]	Total concentration [mM]	Calculated % in solution	Calculated % as neutral complex	Calculated % as charged complex	Calculated total amount bound [mmole g^{-1}]	Measured total amount bound [mmole g^{-1}]
AF	0.30	0.488	0.00	99.92	0.08	0.293	0.30
AF	0.60	0.975	0.00	99.73	0.26	0.586	0.60
AF	1.05	1.750	2.73	54.61	42.69	1.024	1.03
AF	1.23	2.040	8.32	38.58	53.20	1.125	1.11

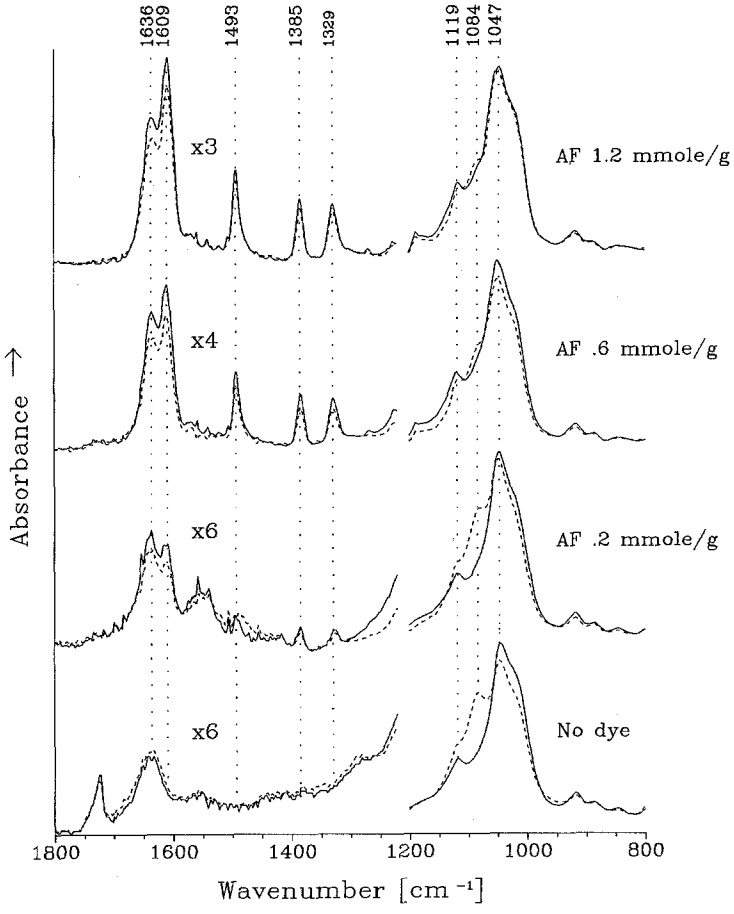

Fig. 1. Linear dichroism-Fourier transform infrared spectra of oriented samples of montmorillonite ("No dye") and AF-montmorillonite complexes with dye amounts as indicated on the right. Dotted lines and full lines indicate 90° and 0° polarization measurements, respectively. Amplification of the range 1200–1800 cm^{-1} is indicated

The XRD measurements [4] show that at low adsorbed amounts of AF, the basal spacing decreases to 1.3 nm, indicating water exclusion from the interlayer space. At added dye amounts higher than 0.3 mmole AF/g clay, the basal spacing increases gradually, reaching 1.55 nm at 0.5 mmole AF/g clay, and 1.62 nm at 1.2 mmole AF/g montmorillonite. The combined information from XRD, LDIR, and adsorption results has enabled us to propose the arrangements of AF molecules in the interlayer space as depicted in Fig. 2. In the absence of the dye, the basal spacing is 1.5 nm (0.95 nm plus at least two layers of water molecules between the plates). The thickness of an AF molecule is about 0.3 nm. At low coverage of AF, water is excluded from the interlayer space and the basal spacing decreases. At higher loading charged complexes are formed (Table 5) and the basal spacing increases (Fig. 2).

Adsorption of divalent organic cations

Figure 3 shows the measured amounts of PQ adsorbed on montmorillonite as a function of total concentration of dye after 1 and 22 days of incubation. Up to the CEC of the clay (equivalent to 0.4 mmole divalent dye per g clay), essentially all the dye adsorbs to the clay. This indicates a very large binding affinity [27, 28]. However, when the amounts added are higher than the CEC, the amounts of PQ adsorbed do not exceed the CEC, unlike the results discussed above for monovalent organic cations. The adsorption reaches equilibrium after less than 1 day.

Competitive adsorption

Figure 4 shows the results of competitive adsorption of PQ and AF at equal concentrations on montmorillonite. The amount of total dyes adsorbed reached a level of 1.1 meq/g. The equivalent amounts of monovalent dye adsorbed were more than those of the divalent dye. There is no decrease in the adsorbed amount of PQ at higher concentrations. It appears that most of the adsorption takes place during the first 24 h of incubation.

We are currently in the stage of further developing the model for simulating the adsorption of divalent organic cations in the presence of several other cations of different valencies. An intriguing result is that above the CEC an increase in the ionic strength reduces the adsorbed amounts of the divalent organic cations studied (unlike the results with monovalent organic cations). In order to gain insight about the interactions of divalent organic cations with the clay mineral, we are currently studying the adsorption, XRD and UV-visible and IR spectra for montmorillonite interacting with the divalent cations PQ, diquat and methyl green (G. Rytwo, S. Nir and L. Margulies, unpublished).

Agro-environmental applications of organo-clays

Specially designed organo-clays can be used for solving environmental problems in modern agriculture, posed for example by the excessive use of pesticides in the field. The application of

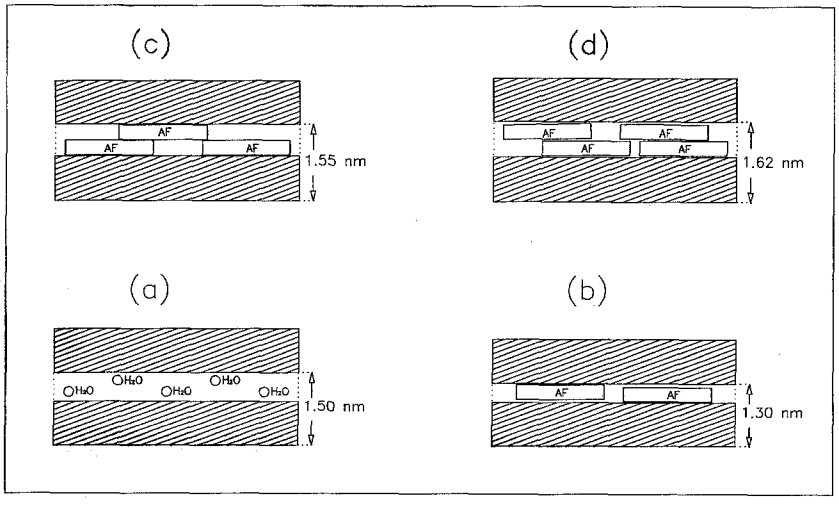

Fig. 2. Illustration of various clay-dye complexes. Shadowed rectangles indicate montmorillonite layers. a): Montmorillonite with no dye, air dried. b): Montmorillonite with 0.2 mmole AF g^{-1} clay. c): Montmorillonite with 0.6 mmole AF g^{-1} clay. d): Montmorillonite with 1.2 mmole AF g^{-1} clay

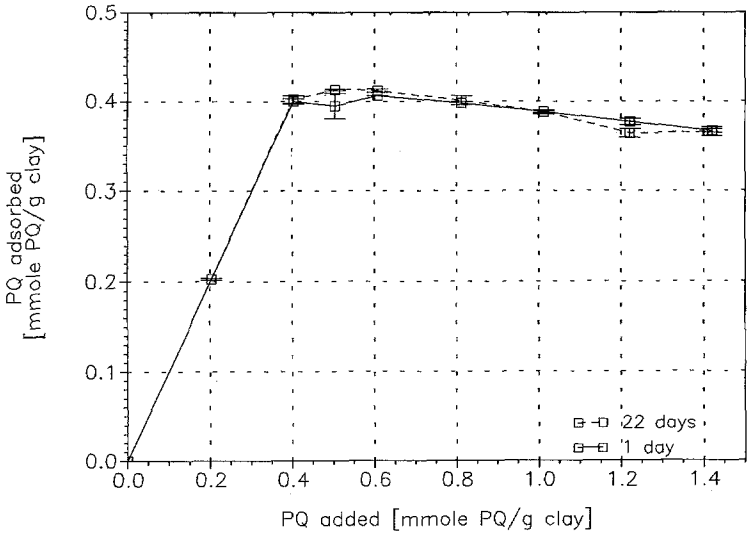

Fig. 3. Adsorption of paraquat (PQ) to montmorillonite after 1 and 22 days of incubation

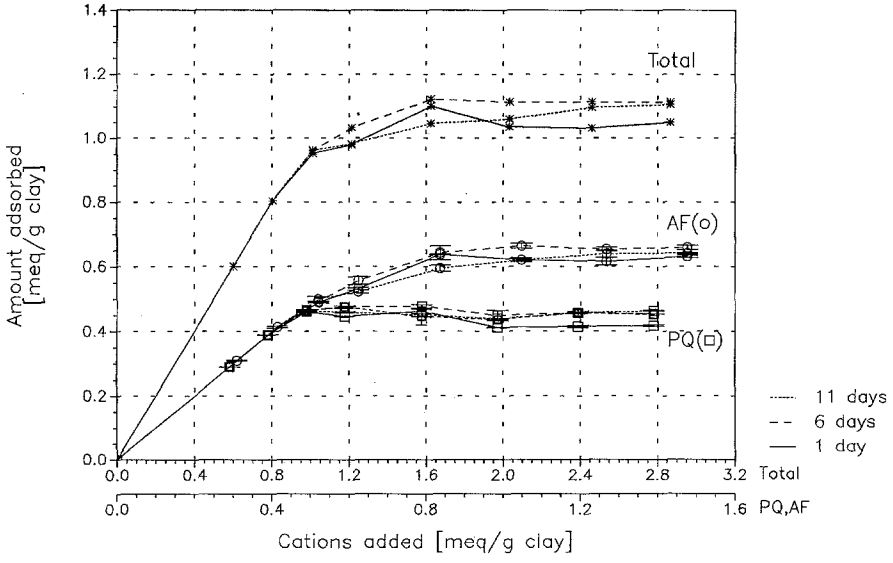

Fig. 4. Competitive adsorption of PQ and acriflavin (AF) to montmorillonite after 1, 6, and 11 days of incubation

pesticides in excess is a common practice in cases where the lifetime of biological activity is shortened either by volatility of such agrochemicals or by their photochemical lability to sunlight.

We have shown that by adsorption of the volatile herbicide S-ethyl dipropyl thiocarbamat (EPTC) to montmorillonite, to sepiolite and to their complexes with the divalent organic cation methyl green, the half-life time of the herbicide was extended to more than 5 days. The half-life time of EPTC in its free form is 10 h. When incorporated into the soil, the half-life times were 4 and 9 days for the free and adsorbed forms, respectively [63].

Photolabile pesticides can be stabilized by adsorbing them on organo-clays containing an additional coadsorbed chromophore. In such systems, efficient energy or charge transfer processes between the photoexcited pesticide (donor) and the chromophore (acceptor) result in an extension of the biological activity of the pesticide, enabling its use in agricultural formulations. The strong attachment of the organic cation to the surface of the clay mineral prevents desorption which might

lead to contamination of soil and water. This approach has been successfully used for photostabilizing both synthetic insecticides and herbicides as well as insecticides of microbial origin [20, 64–69].

Another application of organo-clays is in the development of a method for detoxification of water contaminated with organic pollutants. The method consists of adsorbing the contaminants on organo-clays to which a cationic organic photosensitizer was previously adsorbed, followed by irradiation with visible light. The feasibility of the method was demonstrated by using pentachlorophenol as a model contaminant in water and montmorillonite adsorbed with hexadecyltrimethylammonium with loads above the cation exchange capacity of the clay and with small amounts of methylene blue. After 6 h of irradiation with visible light, the concentration of the toxicant was reduced to less than one-tenth (L. Margulies, S. Pivonia and Y. Chen, unpublished).

In all the above applications, it is of utmost importance to design systems in which clay-organic interactions are optimized to achieve the desired effects. Since these interactions strongly depend on the concentrations of the organic molecules adsorbed, the availability of a theoretical model which can provide the optimal concentrations is important for further improvements in this field.

Acknowledgments

This research was supported by a grant from the Ministry of Science and Technology, Israel, and the Commission of the European Communities.

We thank Ms. Sue Salomon for the expert typing.

References

1. Nir S (1984) J Coll Interface Sci 102:313–321
2. Nir S (1986) Soil Sci Soc Am J 50:52–57
3. Hirsch D, Nir S, Banin A (1989) Soil Sci Soc Am J 53:716–721
4. Rytwo G, Nir S, Margulies L (1994) Soil Sci Soc Am J, (submitted)
5. Baruch E, Lichtenberg D, Barak P, Nir S (1991) Chem Phys Lip 57:17–21
6. Yermiyahu U, Nir S, Ben-Hayyim G, Kafkafi U (1994) J Membr Biol, 138:55–63
7. Newton C, Pangborn W, Nir S, Papahadjopoulos D (1978) Biochim Biophys Acta 506:281–287
8. Nir S, Newton C, Papahadjopoulos D (1978) Bioelectrochem Bioenerg 5:116–133
9. Duzgunes N, Nir S, Wilschut J, Bentz J, Newton C, Portis A, Papahadjopoulos D (1981) J Membr Biol 59:115–125
10. Nir S, Hirsch D, Navrot J, Banin A (1986) Soil Sci Soc Am J 50:40–45
11. Rytwo G, Serban C, Nir S, Margulies L (1991) Clays and Clay Minerals 39:551–555
12. Kurland R, Newton C, Nir S, Papahadjopoulos D (1979) Biochim Biophys Acta 551:137–147
13. Roux M, Bloom M (1990) Biochemistry 29:7077–7089
14. Seelig J, MacDonald PM, Scherer PG (1987) Biochemistry 26:7535–7541
15. Eisenberg M, Gresalfi T, Riccio T, McLaughlin S (1979) Biochemistry 18:5213–5223
16. McLaughlin S, Mulrine N, Gresalfi T, Vaio G, McLaughlin A (1981) J Gen Physiol 77:445–473
17. Ohki S, Ohshima H (1985) Biochim Biophys Acta 812:147–154
18. Dluhy RA, Cameron DG, Mantsch HH, Mendelsohn R (1983) Biochemistry 22:6318–6325
19. Hauser H, Shipley G (1984) Biochemistry 23:34–41
20. Margulies L, Rozen H, Stern T, Rytwo G, Rubin B, Ruzo LO, Nir S, Cohen E (1993) Arch Insect Biochem and Physiol 22:467–486
21. McLaughlin SGA (1977) Curr Top Membr Transp 9:71–144
22. Cenens J, Shoonheydt RA (1988) Clays and Clay Minerals 36:214–224
23. Spencer W, Sutter JR (1979) J Phys Chem 83:1573–1576
24. Nir S, Bentz J, Wilschut J, Duzgunes N (1983) Prog Surface Sci 13:1–124
25. van Olphen H, Fripiat JJ (1979) Data handbook for clay materials and other non-metallic minerals. Pergamon Press, Oxford, p. 19
26. Carter DL, Hilman MD, Gonzales CL (1965) Soil Sci Soc Am Proc 100:356–360
27. Narine DR, Guy RD (1981) Clays and Clay Minerals 29:205–212
28. Margulies L, Rozen H (1986) J Molec Structure 141:219–226
29. Margulies L, Rozen H, Nir S (1988) Clays and Clay Minerals 36:270–276
30. Serratosa JM (1966) Infrared analysis of the orientation of pyridine molecules in clay complexes: in Clays and Clay Minerals, Proc 14th Natl Conf, Berkeley, California, 1965
31. Bentz J, Alford D, Cohen J, Duzgunes N (1988) Biophys J 53:593–607
32. Cohen JA, Cohen M (1981) Biophys J 36:623–651
33. Cohen JA, Cohen M (1984) Biophys J 46:487–490
34. Winiski AP, McLaughlin AC, McDaniel RV, Eisenberg M, McLaughlin S (1986) Biochemistry 25:8206–8214
35. Bentz J, Duzgunes N, Nir S (1983) Biochemistry 22:3320–3330
36. Nir S, Duzgunes N, Bentz J (1983) Biochim Biophys Acta 735:160–172
37. Clarkson DT, Hanson JB (1980) Annu Rev Plant Physiol 31:239–298
38. LaHaye PA, Epstein E (1969) Science 166:395–396
39. Cramer GR, Lauchli A, Polito VS (1985) Plant Physiol 79:207–211

40. Ben Hayyim G, Kafkafi U, Ganmore-Newman R (1987) Plant Physiol 85:434–439
41. Obi I, Ichikawa Y, Kakutani T, Senda M (1989) Plant Cell Physiol 30:129–135
42. McLaughlin A, Eng WK, Vaio G, Wilson T, McLaughlin S (1983) J Membr Biol 76:183–193
43. Lindsay WL (1979) Chemical equilibria in soils. Wiley-Interscience Publ, New York
44. Bentz J (1982) J Coll Interface Sci 90:164–182
45. Portis AR Jr, Newton C, Papahadjopoulos D (1979) Biochemistry 18:780–790
46. Ekerdt R, Papahadjopoulos D (1982) Proc Natl Acad Sci USA 79:2273–2277
47. Sposito G, Holtzclaw KM, Charlet L, Jouany C, Page AL (1983) Soil Sci Soc Am J 47:51–56
48. Lagaly G (1984) Phil Trans R Soc Lond A 311:315–322
49. Lagaly G, Beneke K (1991) Coll Polym Sci 269:1198–1211
50. Mortland MM (1970) Adv Agron 22:75–117
51. Raussel-Colom JA, Serratosa JM (1987) Reactions of clays with organic substances. p. 371–422. In Newman ACD (ed.) Chemistry of clays and clay minerals. Longman Scientifical and Technical, Essex
52. Theng BKG (1974) The chemistry of clay organic reactions. Wiley, New York
53. Yariv S (1988) Intern J Trop Agric 6:1–19
54. Chu CH, Johnson LJ (1979) Clays and Clay Minerals 27:87–90
55. De DK, Das Kanungo JL, Chakravarti SK (1974) Indian J Chem 12:165–166
56. Dobrogowska C, Hepler LG, Ghosh DK, Yariv S (1991) J Thermal Anal 37:1347–1356
57. Ghosal DN, Mukherjee SK (1972) J Indian Chem Soc 49:569–572
58. Grauer Z, Avnir D, Yariv S (1984) Can J Chem 62:1889–1894
59. Hang PT, Brindley GW (1970) Clays and Clay Minerals 18:203–212
60. Venugopal JS, Nair MM (1974) Indian Mineral 15:23–27
61. Yariv S, Lurie D (1971) Israel J Chem 9:537–552
62. Rytwo G, Nir S, Margulies L (1993) Clay Minerals 28:139–143
63. Margulies L, Stern T, Rubin B (1994) J Agric Food Chem, in press
64. Margulies L, Rozen H, Cohen E (1985) Nature 315:658–659
65. Margulies L, Cohen E, Rozen H (1987) Pest Sci 18:79–87
66. Rozen H, Margulies L (1991) J Agric Food Chem 39:1320–1325
67. Margulies L, Stern T, Rubin B, Ruzlo LO (1992) J Agric Food Chem 40:152–155
68. Margulies L, Rozen H, Cohen E (1988) Clays and Clay Minerals 36:159–164
69. Cohen E, Rozen H, Joseph T, Braun S, Margulies L (1990) J Invertebr Pathol 57:343–351

Received February 4, 1994;
accepted February 21, 1994

Authors' address:

Prof. Shlomo Nir
The Seagram Center for Soil and Water Sciences
Faculty of Agriculture
The Hebrew University of Jerusalem
Rehovot 76100, Israel